HHS Public Access

Author manuscript

J Am Chem Soc. Author manuscript; available in PMC 2021 March 16.

Published in final edited form as:

J Am Chem Soc. 2020 September 23; 142(38): 16357–16363. doi:10.1021/jacs.0c06824.

Site-selective RNA Functionalization via DNA-induced Structure

Lu Xiao, **Maryam Habibian**, **Eric T. Kool***

Department of Chemistry, ChEM-H Institute and Stanford Cancer Institute, Stanford University, Stanford, California 94305, United States

Abstract

Methods for RNA functionalization at specific sites are in high demand, but remain a challenge, particularly for RNAs produced by transcription rather than by total synthesis. Recent studies have described acylimidazole reagents that react in high yields at 2′-OH groups stochastically at non-base-paired regions, covering much of the RNA in scattered acyl esters. Localized reactions, if possible, could prove useful in many applications, providing functional handles at specific sites and sequences of the biopolymer. Here we describe a DNA-directed strategy for *in vitro* functionalization of RNA at site-localized 2′-OH groups. The method, RNA Acylation at Induced Loops (RAIL), utilizes complementary helper DNA oligonucleotides that expose gaps or loops at selected positions while protecting the remainder in DNA-RNA duplexes. Reaction with an acylimidazole reagent is then carried out, providing high yields of 2′-OH conjugation at predetermined sites. Experiments reveal optimal helper oligodeoxynucleotide designs and conditions for the reaction, and tests of the approach are carried out to control localized ribozyme activities and to label RNAs with dual-color fluorescent dyes. The RAIL approach offers a simple and novel strategy for site-selective labeling and control of RNAs, potentially of any length and origin.

Graphical Abstract

*Corresponding Author: kool@stanford.edu.

The authors declare no competing financial interest.

ASSOCIATED CONTENT

Supporting Information

The Supporting Information is available free of charge on the ACS Publications website.

Experimental details, spectra, Figure S1–S6 (PDF)

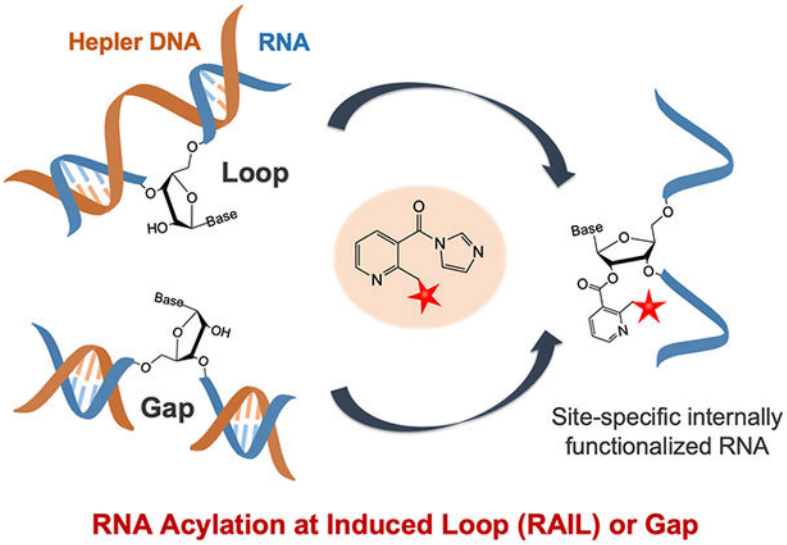

RNA Acylation at Induced Loop (RAIL) or Gap

INTRODUCTION

The complexity of the cellular transcriptome has raised challenges for biologists and chemists to analyze and understand the dynamics, folding and function of many individual RNA species[1–3]. Among the most important chemical strategies for analysis of biopolymers is the development of selective and efficient methods of chemical functionalization. Such methods enable imaging[4], quantification[5], structural analysis[6–8], and immobilization[9], all essential tools in biology and medicine[10–11]. While the development of selective chemical functionalization reactions for proteins has made strong progress over decades[12–13], the development of methods for forming chemical bonds with RNAs remains at an earlier stage. To be sure, total oligonucleotide synthesis enables high levels of control over conjugate design[14–15], but this technology is limited to relatively short RNAs, and is inaccessible to non-specialist laboratories. Among the most significant approaches developed to date for forming bonds with long or transcribed RNAs are enzymatic methods for 5′-end and 3′-end derivatization[16–19], as well as enzymatic approaches applied internally in RNAs that are engineered to contain designed structural domains[10, 20–21]. Also investigated have been methods involving incorporation of unnatural bases via RNA polymerase[22–23], or assisted by catalytic nucleic acids derived from in vitro selection[24–25] or by guide RNA-directed enzymatic modification[26]. Non-enzymatic methods are much more rare, but include 3′-end periodate oxidation followed by reaction of the resulting aldehydes[27–28], which suffers issues with instability.

Methods for bond formation at internal sites in transcribed RNAs remain quite limited or nonselective. DNA-templated generation of 1, N^6-ethenoadenosine derivatives provides a way for site-specific RNA labeling[29–30], but requires intensive synthesis, extended times and long procedures. Diazoketones can be used to react at random phosphates in the chain; however, at internal sites this generates RNA phosphotriester linkages that are hydrolytically

unstable[31–32]. Photocrosslinkers such as psoralens are selective only for double-stranded regions in folded RNAs, and are used not for specific functionalization, but rather in low yields for structural mapping[33]. Base-reactive agents such as dimethylsulfate, which reacts at cytosine and adenine, or ninhydrin, which reacts at guanine[34], show only selectivity for unpaired bases over paired ones[35], and block base pairing. Finally, a number of acylating reagents that form bonds at 2′-OH groups of unpaired nucleotides have been widely used in trace yields for structural mapping[36–37]; however, these are typically unsuitable for high-yield functionalization due to their low solubility and very high reactivity. Importantly, no method for sequence- or site-selective reaction has been reported for any of these essentially stochastic reactions.

Recent studies have shown that increasing the solubility and lowering the reactivity of acylating agents can increase yields of 2′-OH ester formation with RNA to stoichiometric and even superstoichiometric levels[38–43]. A number of acylimidazole reagents have been shown to functionalize RNA at high yields, enabling efficient labeling and caging of transcribed RNAs[41, 44–45]. Similarly, isatoic anhydride reagents have recently been detuned and solubilized to increase functional yields for potential applications such as separation of RNA from DNA[46–47]. To date, however, these acylation reactions are nonselective among single-stranded regions of RNA, and so RNAs of interest contain many possible sites of reaction. This nonselective polyacylation can result, for some applications, in undesired blocking of binding folding, and function, and places limits on the development of caging strategies. Despite the increasing utility of 2'-OH acylation[48], there remains no method for directing esterification to specific RNA sites.

Here we address this selectivity issue by developing a versatile strategy for site-localized acylation of RNAs. The method, RNA Acylation at Induced Loops (RAIL), takes advantage of the low reactivity of RNAs in double-stranded structure by use of complementary DNA oligonucleotides to protect all but the desired reaction sites in an RNA. We show that reactive gaps or loops in the RNA can be induced by appropriately designed and inexpensive helper DNAs, resulting in high yields of acylation at predetermined sites. The sequence-selective reaction occurs with near-nucleotide resolution, and allows for subsequent RNA labeling and control. We expect that the RAIL approach will be broadly applicable to many RNA species, and should be accessible to many chemistry and biology laboratories.

RESULTS

Structural design for site-selective RNA acylation.

To test the possibility of site-selective RNA acylation, we constructed duplex structures containing a loop or a gap at a predetermined RNA site by the use of designed helper DNAs (Figure 1). The helper DNAs (H) are complementary to the RNA of interest (R) with one or more nucleotides omitted at a predetermined position. Hybridization should then leave selected ribonucleotides unpaired at this site. For chemical functionalization, a water-soluble nicotinyl acylimidazole compound (NAI-N_3), previously shown to polyacylate RNAs[39], was adopted as the test acylating reagent. We hypothesized that the complementary DNA could suppress RNA acylation at otherwise reactive positions by protecting the 2′-OH groups within duplex structure, which mapping studies have shown to be less reactive[7]. Conversely,

designing the helper DNAs to induce loops or leave unpaired gaps would be expected to expose specific RNA 2′-OH groups to promote acylation at designed sites. After DNA removal, the selectively functionalized RNA could be obtained and employed in further applications.

Performance of DNA-RNA duplex protection.

To test our proposed strategy, we first aimed to determine the extent to which a complementary DNA can protect an RNA from 2'-OH acylation. Literature studies[7, 37] of RNA acylation during structure mapping have established that duplex RNAs are protected relative to single-stranded sequences, but the degree of selectivity is less well characterized, particularly under high reagent concentrations necessary for stoichiometric levels of reaction. Moreover, there appears to exist no data on whether a RNA-DNA hybrid is protected similarly to purely double-stranded RNA. To test these issues, we initially studied the performance of DNA protection with a 39nt RNA model sequence derived from a biological miRNA target (Tables S1, S2). We compared the reactions of the known high-yielding (and functionalizable)[7] acylating agent NAI-N_3 with the single-stranded RNA (ssRNA) and with a pre-annealed RNA-DNA duplex by MALDI-TOF mass spectrometry to observe numbers of adducts (Figure 2a). 5 μM ssRNA or RNA-DNA duplex was reacted with 50 mM NAI-N_3 at 37°C for 4 h in MOPS buffer, after which DNase I was added to remove the protecting DNA, and the reacted RNA was then isolated by ethanol precipitation. Importantly, we found that in comparison to ssRNA (R), which was functionalized with an average of six acyl groups (up to 25% of 2′-OH groups) under these conditions, the acylation of RNA protected by fully complementary DNA (R/H duplex) was dramatically reduced to a range of 0 to 2 groups (Figure 2b). We hypothesized that some of the observed acylation of this DNA-protected RNA might potentially occur at the ends of the RNA, since the 5′-, 2′-, and 3′-OH groups may not be efficiently protected in the blunt-ended duplex structure. To test whether the end protection could be improved, we added three-base deoxyadenosine (A_3) overhangs at both ends of the DNA (H_o), expecting to stabilize the helix (R/H_o) at the RNA ends via the stacking effects of the dangling residues[49]. Gratifyingly, this resulted in reducing acylation yields to an average of ~0.3 acyl groups in the RNA (Figure 2b). It was not clear whether this small amount of remaining acylation occurs at the 5′ or 3′ end of the RNA, or from residual low reactivity within the duplex region. To test this, we carried out reactions with duplexes (R_p/H_o) in which the 2'- and 3'-OH groups at 3′ end of RNA were omitted by replacement of the terminal nucleotide with a deoxynucleoside with a 3′-phosphate group (R_p); this resulted in almost complete loss of observed adduct peaks in the mass spectrum after reaction (Figure 2b). This establishes that the 5′-OH group is less susceptible to acylation than the hydroxyls at the 3′ end of RNA (Figure 2b, S1a). In addition, the A_3 overhang DNA protection also worked well with a higher NAI-N_3 concentration (Figure S1b), which can enable higher stoichiometric yields at the intended residues. Overall, the experiments revealed that a simple, unmodified overhang helper DNA can efficiently protect an RNA from highly acylating conditions, suppressing reactivity at a given internal 2′-OH group by at least ca. 30-fold as judged by mass spectrometry.

The mass spectrometry data gives useful information about yields, but not position, of acylation. To determine positions of trace acylation, we carried out studies using denaturing polyacrylamide gel electrophoresis (PAGE) after a reverse transcriptase (RT) extension of a primer hybridized to the end of the RNA. As in SHAPE structure mapping experiments[7], the adduct blocks RT elongation at the modified nucleotide, which results in cDNA truncation observable on the gel. The gel analysis allowed us to monitor positions of acylation at nucleotide resolution calibrated with sequencing lanes (Figure 2c). In accordance with the mass data, most RNA-DNA duplex samples (R/H, R/H_o, R_p/H_o) were successfully reverse transcribed into full-length cDNA while the unprotected and acylated ssRNA (R) was stopped at the initial stage, supporting the high performance of DNA protection in the duplex (Figure 1c). The protected R/H, R/H_o and R_p/H_o duplexes gave only trace acylation within the body of the RNA, adding support to the prior finding that the differences in mass described above resulted primarily from small amounts of reaction at the RNA terminus. Two bands of slightly higher trace acylation were visible at central C, U sites compared with mock treated RNA control, which might be due to local sequence-dependent flexibility or alternative structure in the RNA-DNA duplex.

RNA acylation at induced loops (RAIL).

Encouraged by the data showing successful DNA protection of RNA from random acylation, we next evaluated whether it is possible to restore reactivity at designed locations in the RNA by further engineering of the helper DNA. First, we tested the possibility of inducing a loop by omitting one or more nucleotides in the helper DNA, which would be expected to result in an RNA bulge loop (Figure 3a). Tests with a DNA helper designed to induce a 1nt RNA bulge (R_p/H_o-L1) to optimize reaction conditions showed a high-yield localized RNA acylation at position “U” with 200 mM NAI-N_3 for 4 h at 37 °C (Figure S2). To test the efficiency and site specificity of RAIL, reactions with no loop (R/H_o vs. R_p/H_o), 1nt bulge (R/Ho-L1 vs. Rp/Ho-L1) and 3nt loop (R/Ho-L3 vs. Rp/Ho-L3) RNA-DNA duplexes were compared. We examined the prior 2′-deoxy-3′-phosphate modified 39mer RNA (Rp) for mass studies. The data showed a median of one adduct (range 0–2) in 1nt bulge RNA (Rp/Ho-L1) and two adducts (range 1–3) in 3nt loop RNA (Rp/Ho-L3) (Figure 3b). PAGE gel analysis (Figure 3c, S3) with reverse transcriptase primer extension for the 1nt bulge revealed that the darkest band appeared at G, which is the position corresponding to RT stopping immediately before the acylated nucleotide. This establishes that the acylation occurs primarily at the intended bulged U residue. For the trinucleotide loop, the acylated sites were concentrated at the 3nt CUG loop sites as expected. Interestingly, in both cases there was also a small amount of acylation at the adjacent nucleotide 5′ to the induced loop, which is explainable by added accessibility of this 2′-OH next to the bulge. Preliminary kinetics experiments revealed that the ratio of the acylation at the primary and secondary site 2′-OH groups remained constant over time (Figure S2e).

RNA acylation at an induced gap.

We proceeded to study whether the localized RNA acylation could also be achieved at an induced gap position. Two strands of helper DNAs were exploited to bind adjacent to make a nicked duplex (R/H_o-N vs. R_p/H_o-N), or slightly separated to render a 1nt gap at U (R/H_o-G1 vs. R_p/H_o-G1) and 3nt gap at GCU (R/H_o-G3 vs. R_p/H_o-G3) (Figure 4a). The duplexes

were reacted as before with 200 mM NAI-N_3 at 37°C in MOPS buffer. The acylation yields on RNA were found to increase from intact duplex < nick< 1nt gap < 3nt gap reactions as shown by mass spectrometry data (Figure S4). We measured the acylation positions in these cases via RT stops and again observed reaction centered at the designed gaps (Figure 4b). Notably, the nicked duplex case showed very little acylation, which supports prior observations that nicked duplexes remain largely stacked and stable[50]. Overall, we conclude that adjacently-hybridized helper DNAs are highly effective in protecting an RNA from acylation, and that a 1-nt gap left between the DNAs can result in site-selective acylation with efficiency and selectivity near that induced by a 1-nt bulge.

Programming the position of acylation.

After confirming that RNA acylation can be restricted to a loop or gap position, we tested the generality of predetermining selected reaction positions using these methods. We employed new helper DNAs to shift a putative 1nt bulge or gap from U to G, C, A at progressively further locations downstream from the primer in the 39mer RNA, and measured the RT stops after acylation, DNA removal and ethanol precipitation (Figure 5). The data show clearly that the RT stops were shifted with the moving loops or gaps, establishing programmability of the method, and confirming that loops of any of the four ribonucleotides can be acylated. Interestingly, the induced gap experiments showed poor selectivity at positions near the end, which might be expected as one helper DNA became too short to hybridize well under the reaction conditions. The induced loop cases did not show this issue, likely due to the long length of the single helper.

Site-selective control of a tandem ribozyme.

Having established conditions and helper designs that yield strong protection and efficient site selectivity, we then proceeded to test the practical utility of the approach for acylation-based control of a tandem ribozyme. Although previous studies have described methods for control of a single catalytic RNA[51–54], the use of a tandem ribozyme (TR) here offered the possibility to selectively control one RNA function relative to another within the same strand. An 81nt tandem hammerhead ribozyme with dual catalytic cores (3TR and 5TR) was produced by *in vitro* transcription and was reacted under site-selective conditions at their catalytic cores by the RAIL method under the standard conditions (Figure 6a, S6a; see SI for details). The dual catalytic activities of the TRs were measured through fluorescence enhancements by incubation with two doubly labeled reporter substrates containing a fluorophore and a quencher (3S and 5S) in 50 mM Tris pH 7.5, 10 mM $MgCl_2$ (Figure 6b). The untreated TR displayed strong dual substrate cleaving activities toward 3S and 5S, giving pronounced emission at both 520 nm and 665 nm (Figure S5). The 3TR-acylated ribozyme showed a strong fluorescence at 665 nm but relatively little at 520 nm, indicating successful and selective acylation at the 3TR site while conserving activity at the helper-protected site. Conversely, the 5TR-acylated ribozyme using the alternative RAIL helper generated intense fluorescence at 520 nm, but weak emission at 665 nm. Analysis of the tandem ribozyme reaction rates revealed that 3TR acylation suppressed the rate of 3S cleavage by ~5-fold and retained ca. 85% of the initial rate of untreated TR with the 5TR substrate; similarly, the initial cleavage rates of 5TR-acylated ribozyme were decreased by 4-fold for 5S, while 3TR-ribozyme activity remained at 93% levels relative to untreated TR

(Figure 6c). These results establish that RNA acylation can be locally programmed via RAIL in a multifunctional RNA, resulting in high yields of acylation-based suppression at the intended site, while giving relatively little off-target acylation at the remaining sites.

Dual labeling of small nucleolar RNA for FRET via successive RAIL labeling.

The above experiments confirmed the ability of RAIL to direct site-localized suppression of one local function of a larger RNA containing multiple active sites. Next, we tested whether RAIL could be used in successive fashion on a single RNA for a dual labeling experiment. NAI-N_3 contains both an acylimidazole group for acylation and an azide group that can react with alkynes via cycloaddition. For these experiments, we chose the 65nt small nucleolar RNA, SNORD78, which has been shown to act as an oncogene in lung cancer[55–56] and is associated with hepatocellular carcinoma[57] and prostate cancer[58] as an enhancer for proliferation, migration and invasion. Dual labeling has been employed in synthetic DNAs and RNAs for structural studies via FRET-enabled distance measurements, but it is much more challenging to engineer a transcribed RNA to contain two labels at internal positions.

To test dual labeling of SNORD78 RNA, we introduced the fluorophore Alexa488 at the 2′-OH of G14 and fluorophore TAMRA at A49 by two RAIL reactions (Figure 7a, S6b). The labeling was carried out successively, emplacing one DNA-directed acyl group, reacting it with the first fluorescent label, then carrying out the second RAIL-directed acylation with a second DNA helper and labeling in analogous fashion. The gel analysis confirmed the presence of both labels by the overlapping fluorescent signals of both fluorophores (Figure 7b). Labeling efficiency was sufficient to show a robust FRET signal between the dyes, and to register a drop-in energy transfer upon denaturing the structure in low-salt conditions (Figure 7c). These results suggest that the RAIL method can offer high utility in the study of RNA structure, and more generally in RNA labeling. Notably, it requires no introduction of nonnative sequences, and only knowledge of the RNA sequence is needed to carry it out.

DISCUSSION

Our experiments introduce a novel strategy for site-directed stoichiometric acylation of RNAs produced by chemical synthesis or by transcription. The RAIL method is rapid, requiring only a few hours to yield the functionalized RNA, and its simplicity should render it accessible to chemistry and biology researchers alike. Since acylation with NAI-N_3 has been used both for blocking and caging[39] as well as click-based conjugation[7], the method can yield functional blocking groups, caging groups, affinity labels and fluorescent labels at desired positions internally in RNA at high resolution. Also important is the feature that NAI-N_3 generates a reversible adduct on RNA; chemical treatment with phosphines *in vitro* or *in vivo* rapidly removes this group, restoring RNA structure and function. Thus, RAIL could be used to introduce caging groups at designed sites in transcribed RNAs without engineering non-native sequence or structure into the RNAs, which may interfere with biological activity. Our results also show that RAIL can be performed serially on an RNA, introducing multiple distinct labels in high yields at separate sites. The cost of the approach is low, given that DNA oligonucleotides are rapidly available at modest prices, and DNase is also widely available for removal of helper DNAs.

One limitation of the RAIL approach is the need for stable hybridization of the loop-inducing DNA, which may restrict its use in very short RNAs (shorter than ca. 12nt) due to poor binding of helper DNAs. It is possible that helper DNAs with strongly-binding modifications may aid in addressing this issue. On the opposite end of the spectrum, it is worth considering the use of the method with RNAs longer than the available length of synthetic DNA helpers. Although synthesized DNA oligonucleotides are typically limited in length to ~150–200nt, in principle the method could be carried out with RNAs of longer lengths by use of long enzymatically produced helper DNAs,[59] or by tiling synthesized helper DNAs along a strand as done in our nick experiments. Future research will be needed to test this possibility. A second limitation is that placement of acyl groups at 1nt bulges or gaps by RAIL is not completely homogeneous, giving small amounts of secondary acylation (estimated at ~20–30%; see Figure 3c and discussion in Fig. S2) at the adjacent position. In many applications, this may not be a serious issue, given the close positioning of the secondary adducts. Similar utility is found with labeled antibodies where mixtures of labeled conjugates are widely useful. However, when complete RNA homogeneity is required for an experiment it is a limitation worth considering. It is possible that modification of the helper DNAs near this site may aid in suppressing this secondary acylation. Future experiments will address this issue.

Supplementary Material

Refer to Web version on PubMed Central for supplementary material.

ACKNOWLEDGMENT

We thank the U.S. National Institutes of Health (GM127295 and GM130704) for support.

REFERENCES

(1). He C, Grand Challenge Commentary: RNA epigenetics? Nat. Chem. Biol 2010, 6 (12), 863–865. [PubMed: 21079590]

(2). Wan Y; Kertesz M; Spitale RC; Segal E; Chang HY, Understanding the transcriptome through RNA structure. Nat. Rev. Genet 2011, 12 (9), 641–655. [PubMed: 21850044]

(3). Cech Thomas R.; Steitz Joan A., The Noncoding RNA Revolution-Trashing Old Rules to Forge New Ones. Cell 2014, 157 (1), 77–94. [PubMed: 24679528]

(4). Pichon X; Lagha M; Mueller F; Bertrand E, A Growing Toolbox to Image Gene Expression in Single Cells: Sensitive Approaches for Demanding Challenges. Mol. Cell 2018, 71 (3), 468–480. [PubMed: 30075145]

(5). Rabani M; Levin JZ; Fan L; Adiconis X; Raychowdhury R; Garber M; Gnirke A; Nusbaum C; Hacohen N; Friedman N; Amit I; Regev A, Metabolic labeling of RNA uncovers principles of RNA production and degradation dynamics in mammalian cells. Nat. Biotechnol 2011, 29 (5), 436–442. [PubMed: 21516085]

(6). Bokinsky G; Rueda D; Misra VK; Rhodes MM; Gordus A; Babcock HP; Walter NG; Zhuang X, Single-molecule transition-state analysis of RNA folding. Proc. Natl. Acad. Sci. U.S.A 2003, 100 (16), 9302. [PubMed: 12869691]

(7). Spitale RC; Flynn RA; Zhang QC; Crisalli P; Lee B; Jung J-W; Kuchelmeister HY; Batista PJ; Torre EA; Kool ET; Chang HY, Structural imprints in vivo decode RNA regulatory mechanisms. Nature 2015, 519 (7544), 486–490. [PubMed: 25799993]

(8). Liu Y; Holmstrom E; Yu P; Tan K; Zuo X; Nesbitt DJ; Sousa R; Stagno JR; Wang Y-X, Incorporation of isotopic, fluorescent, and heavy-atom-modified nucleotides into RNAs by position-selective labeling of RNA. Nat. Protoc 2018, 13 (5), 987–1005. [PubMed: 29651055]

(9). Vioque A; Altman S, Affinity chromatography with an immobilized RNA enzyme. Proc. Natl. Acad. Sci. U.S.A 1986, 83 (16), 5904. [PubMed: 3526344]

(10). Li F; Dong J; Hu X; Gong W; Li J; Shen J; Tian H; Wang J, A Covalent Approach for Site-Specific RNA Labeling in Mammalian Cells. Angew. Chem. Int. Ed 2015, 54 (15), 4597–4602.

(11). Zhang D; Zhou CY; Busby KN; Alexander SC; Devaraj NK, Light-Activated Control of Translation by Enzymatic Covalent mRNA Labeling. Angew. Chem. Int. Ed 2018, 57 (11), 2822–2826.

(12). Spicer CD; Davis BG, Selective chemical protein modification. Nat. Commun 2014, 5 (1), 4740. [PubMed: 25190082]

(13). Boutureira O; Bernardes GJL, Advances in Chemical Protein Modification. Chem. Rev 2015, 115 (5), 2174–2195. [PubMed: 25700113]

(14). Allerson CR; Chen SL; Verdine GL, A Chemical Method for Site-Specific Modification of RNA: The Convertible Nucleoside Approach. J. Am. Chem. Soc 1997, 119 (32), 7423–7433.

(15). Fauster K; Hartl M; Santner T; Aigner M; Kreutz C; Bister K; Ennifar E; Micura R, 2′-Azido RNA, a Versatile Tool for Chemical Biology: Synthesis, X-ray Structure, siRNA Applications, Click Labeling. ACS Chem. Biol 2012, 7 (3), 581–589. [PubMed: 22273279]

(16). England TE; Uhlenbeck OC, 3′-Terminal labelling of RNA with T4 RNA ligase. Nature 1978, 275 (5680), 560–561. [PubMed: 692735]

(17). Paredes E; Das SR, Click Chemistry for Rapid Labeling and Ligation of RNA. ChemBioChem 2011, 12 (1), 125–131. [PubMed: 21132831]

(18). Schulz D; Holstein JM; Rentmeister A, A Chemo-Enzymatic Approach for Site-Specific Modification of the RNA Cap. Angew. Chem. Int. Ed 2013, 52 (30), 7874–7878.

(19). Samanta B; Horning DP; Joyce GF, 3′-End labeling of nucleic acids by a polymerase ribozyme. Nucleic Acids Res. 2018, 46 (17), e103–e103. [PubMed: 29901762]

(20). McDonald RI; Guilinger JP; Mukherji S; Curtis EA; Lee WI; Liu DR, Electrophilic activity-based RNA probes reveal a self-alkylating RNA for RNA labeling. Nat. Chem. Biol 2014, 10 (12), 1049–1054. [PubMed: 25306441]

(21). Alexander SC; Busby KN; Cole CM; Zhou CY; Devaraj NK, Site-Specific Covalent Labeling of RNA by Enzymatic Transglycosylation. J. Am. Chem. Soc 2015, 137 (40), 12756–12759. [PubMed: 26393285]

(22). Kawai R; Kimoto M; Ikeda S; Mitsui T; Endo M; Yokoyama S; Hirao I, Site-Specific Fluorescent Labeling of RNA Molecules by Specific Transcription Using Unnatural Base Pairs. J. Am. Chem. Soc 2005, 127 (49), 17286–17295. [PubMed: 16332078]

(23). Liu Y; Holmstrom E; Zhang J; Yu P; Wang J; Dyba MA; De C; Ying J; Lockett S; Nesbitt DJ; Ferré-D'Amaré AR; Sousa R; Stagno JR; Wang Y-X, Synthesis and applications of RNAs with position-selective labelling and mosaic composition. Nature 2015, 522 (7556), 368–372. [PubMed: 25938715]

(24). Baum DA; Silverman SK, Deoxyribozyme-Catalyzed Labeling of RNA. Angew. Chem. Int. Ed 2007, 46 (19), 3502–3504.

(25). Ghaem Maghami M; Scheitl CPM; Höbartner C, Direct in Vitro Selection of Trans-Acting Ribozymes for Posttranscriptional, Site-Specific, and Covalent Fluorescent Labeling of RNA. J. Am. Chem. Soc 2019, 141 (50), 19546–19549. [PubMed: 31778306]

(26). Tomkuvienė M; Clouet-d'Orval B; Černiauskas I; Weinhold E; Klimašauskas S, Programmable sequence-specific click-labeling of RNA using archaeal box C/D RNP methyltransferases. Nucleic Acids Res. 2012, 40 (14), 6765–6773. [PubMed: 22564896]

(27). Bellon L; Workman C; Scherrer J; Usman N; Wincott F, Morpholino-Linked Ribozymes: A Convergent Synthetic Approach. J. Am. Chem. Soc 1996, 118 (15), 3771–3772.

(28). Yamamoto J; Ebisuda S; Kong L; Yamago H; Iwai S, Post-synthetic Modification of 3′ Terminus of RNA with Propargylamine: A Versatile Scaffold for RNA Labeling through Copper-catalyzed Azide-Alkyne Cycloaddition. Chem. Lett 2017, 46 (5), 767–770.

(29). Egloff D; Oleinich IA; Zhao M; König SLB; Sigel RKO; Freisinger E, Sequence-Specific Post-Synthetic Oligonucleotide Labeling for Single-Molecule Fluorescence Applications. ACS Chem. Biol 2016, 11 (9), 2558–2567. [PubMed: 27409145]

(30). Zhao M; Steffen FD; Börner R; Schaffer MF; Sigel Roland K O.; Freisinger E, Site-specific dual-color labeling of long RNAs for single-molecule spectroscopy. Nucleic Acids Res. 2017, 46 (3), e13–e13.

(31). Ando H; Furuta T; Tsien RY; Okamoto H, Photo-mediated gene activation using caged RNA/DNA in zebrafish embryos. Nat. Genet. 2001, 28 (4), 317–325. [PubMed: 11479592]

(32). Blidner RA; Svoboda KR; Hammer RP; Monroe WT, Photoinduced RNA interference using DMNPE-caged 2′-deoxy-2′-fluoro substituted nucleic acidsin vitro and in vivo. Mol. Biosyst. 2008, 4 (5), 431–440. [PubMed: 18414741]

(33). Lu Z; Zhang Qiangfeng C.; Lee B; Flynn Ryan A.; Smith Martin A.; Robinson James T.; Davidovich C; Gooding Anne R.; Goodrich Karen J.; Mattick John S.; Mesirov Jill P.; Cech Thomas R.; Chang Howard Y., RNA Duplex Map in Living Cells Reveals Higher-Order Transcriptome Structure. Cell 2016, 165 (5), 1267–1279. [PubMed: 27180905]

(34). Wang S-R; Huang H-Y; Liu J; Wei L; Wu L-Y; Xiong W; Yin P; Tian T; Zhou X, The Manipulation of RNA-Guided Nucleic Acid Cleavage with Ninhydrin Chemistry. Advanced Science 2020, 7 (13), 1903770. [PubMed: 32670753]

(35). Graveley BR, RNA Matchmaking: Finding Cellular Pairing Partners. Mol. Cell 2016, 63 (2), 186–189. [PubMed: 27447984]

(36). Merino EJ; Wilkinson KA; Coughlan JL; Weeks KM, RNA Structure Analysis at Single Nucleotide Resolution by Selective 2'-Hydroxyl Acylation and Primer Extension (SHAPE). J. Am. Chem. Soc 2005, 127 (12), 4223–4231. [PubMed: 15783204]

(37). Spitale RC; Flynn RA; Torre EA; Kool ET; Chang HY, RNA structural analysis by evolving SHAPE chemistry. WIREs RNA 2014, 5 (6), 867–881. [PubMed: 25132067]

(38). Nodin L; Noël O; Chaminade F; Maskri O; Barbier V; David O; Fossé P; Xie J, RNA SHAPE chemistry with aromatic acylating reagents. Biorg. Med. Chem. Lett 2015, 25 (3), 566–570.

(39). Kadina A; Kietrys AM; Kool ET, RNA Cloaking by Reversible Acylation. Angew. Chem. Int. Ed 2018, 57 (12), 3059–3063.

(40). Velema WA; Kool ET, Water-Soluble Leaving Group Enables Hydrophobic Functionalization of RNA. Org. Lett 2018, 20 (20), 6587–6590. [PubMed: 30299958]

(41). Velema WA; Kietrys AM; Kool ET, RNA Control by Photoreversible Acylation. J. Am. Chem. Soc 2018, 140 (10), 3491–3495. [PubMed: 29474085]

(42). Park HS; Kietrys AM; Kool ET, Simple alkanoyl acylating agents for reversible RNA functionalization and control. Chem. Commun 2019, 55 (35), 5135–5138.

(43). Habibian M; Velema WA; Kietrys AM; Onishi Y; Kool ET, Polyacetate and Polycarbonate RNA: Acylating Reagents and Properties. Org. Lett 2019, 21 (14), 5413–5416. [PubMed: 31268332]

(44). Habibian M; McKinlay C; Blake TR; Kietrys AM; Waymouth RM; Wender PA; Kool ET, Reversible RNA acylation for control of CRISPR–Cas9 gene editing. Chem. Sci 2020, 11 (4), 1011–1016.

(45). Wang S-R; Wu L-Y; Huang H-Y; Xiong W; Liu J; Wei L; Yin P; Tian T; Zhou X, Conditional control of RNA-guided nucleic acid cleavage and gene editing. Nat. Commun 2020, 11 (1), 91. [PubMed: 31900392]

(46). Ursuegui S; Chivot N; Moutin S; Burr A; Fossey C; Cailly T; Laayoun A; Fabis F; Laurent A, Biotin-conjugated N-methylisatoic anhydride: a chemical tool for nucleic acid separation by selective 2′-hydroxyl acylation of RNA. Chem. Commun 2014, 50 (43), 5748–5751.

(47). Ursuegui S; Yougnia R; Moutin S; Burr A; Fossey C; Cailly T; Laayoun A; Laurent A; Fabis F, A biotin-conjugated pyridine-based isatoic anhydride, a selective room temperature RNA-acylating agent for the nucleic acid separation. Org. Biomol. Chem 2015, 13 (12), 3625–3632. [PubMed: 25671759]

(48). Velema WA; Kool ET, The chemistry and applications of RNA 2′-OH acylation. Nat. Rev. Chem 2020, 4 (1), 22–37. [PubMed: 32984545]

(49). Sugimoto N; Kierzek R; Turner DH, Sequence dependence for the energetics of dangling ends and terminal base pairs in ribonucleic acid. Biochemistry 1987, 26 (14), 4554–4558. [PubMed: 2444250]

(50). Protozanova E; Yakovchuk P; Frank-Kamenetskii MD, Stacked–Unstacked Equilibrium at the Nick Site of DNA. J. Mol. Biol 2004, 342 (3), 775–785. [PubMed: 15342236]

(51). Chaulk SG; MacMillan AM, Caged RNA: photo-control of a ribozyme reaction. Nucleic Acids Res. 1998, 26 (13), 3173–3178. [PubMed: 9628915]

(52). Wang DY; Lai BHY; Sen D, A General Strategy for Effector-mediated Control of RNA-cleaving Ribozymes and DNA Enzymes. J. Mol. Biol 2002, 318 (1), 33–43. [PubMed: 12054766]

(53). Young DD; Deiters A, Photochemical hammerhead ribozyme activation. Biorg. Med. Chem. Lett 2006, 16 (10), 2658–2661.

(54). Savinov A; Block SM, Self-cleavage of the glmS ribozyme core is controlled by a fragile folding element. Proc. Natl. Acad. Sci. U.S.A 2018, 115 (47), 11976. [PubMed: 30397151]

(55). Zheng D; Zhang J; Ni J; Luo J; Wang J; Tang L; Zhang L; Wang L; Xu J; Su B; Chen G, Small nucleolar RNA 78 promotes the tumorigenesis in non-small cell lung cancer. J. Exp. Clin. Cancer Res 2015, 34 (1), 49. [PubMed: 25975345]

(56). Su J; Liao J; Gao L; Shen J; Guarnera MA; Zhan M; Fang H; Stass SA; Jiang F, Analysis of small nucleolar RNAs in sputum for lung cancer diagnosis. Oncotarget 2016, 7 (5), 5131–5142. [PubMed: 26246471]

(57). Ma P; Wang H; Han L; Jing W; Zhou X; Liu Z, Up-regulation of small nucleolar RNA 78 is correlated with aggressive phenotype and poor prognosis of hepatocellular carcinoma. Tumor Biol. 2016, 37 (12), 15753–15761.

(58). Martens-Uzunova ES; Hoogstrate Y; Kalsbeek A; Pigmans B; den Berg M. V.-v.; Dits N; Nielsen SJ; Baker A; Visakorpi T; Bangma C; Jenster G, C/D-box snoRNA-derived RNA production is associated with malignant transformation and metastatic progression in prostate cancer. Oncotarget 2015, 6 (19).

(59). Hao M; Qiao J; Qi H, Current and Emerging Methods for the Synthesis of Single-Stranded DNA. Genes 2020, 11 (2).

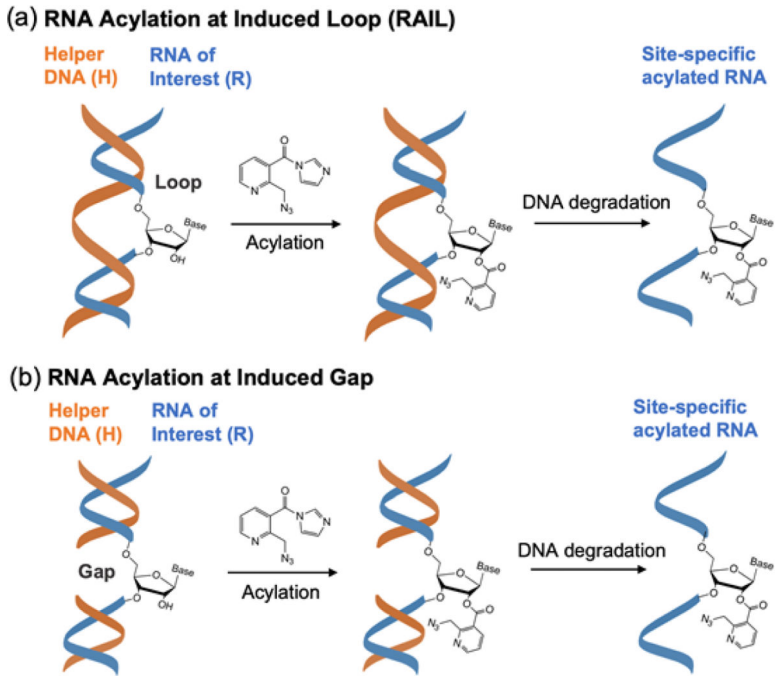

Figure 1.

Schematic of the RAIL approach for site-selective RNA acylation. The RNA of interest (R) is incubated with one or more complementary helper DNAs (H) to protect most of the RNA, but leaving a single unpaired nucleotide in a loop (a) or gap (b). The exposed 2′-OH group can then selectively react with an acylating reagent, such as the prototypical NAI-N_3, yielding a site-defined functionalized RNA after removing the helper DNA. Note that loops and gaps larger than a single nucleotide are also possible.

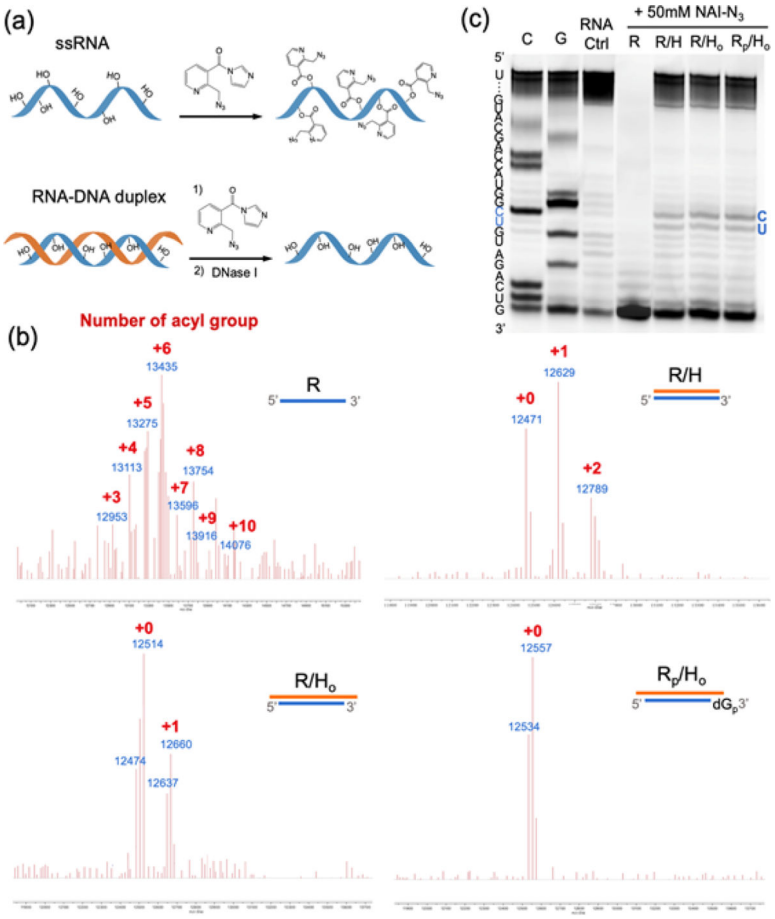

Figure 2.

Optimizing helper DNA protection from random RNA acylation. (a) Schematic of acylation of single stranded RNA (ssRNA) and RNA-DNA duplex with a full DNA complement. (b) MALDI-TOF mass spectrum of acylated ssRNA (R), RNA protected by fully complementary DNA (R/H), RNA protected by fully complementary DNA with three deoxyadenosines overhanging at both ends (R/H$_o$) and 2′-deoxy-3′-phosphate modified RNA protected by fully complementary DNA with 3a overhang (R$_p$/H$_o$); reacting with 50 mM NAI-N3 at 37°C for 4h in MOPS buffer. (c) Gel electrophoretic analysis of reverse transcriptase (RT) primer extension reveals a general lack of stops due to protected RNA, save for trace reaction at a central C, U site.

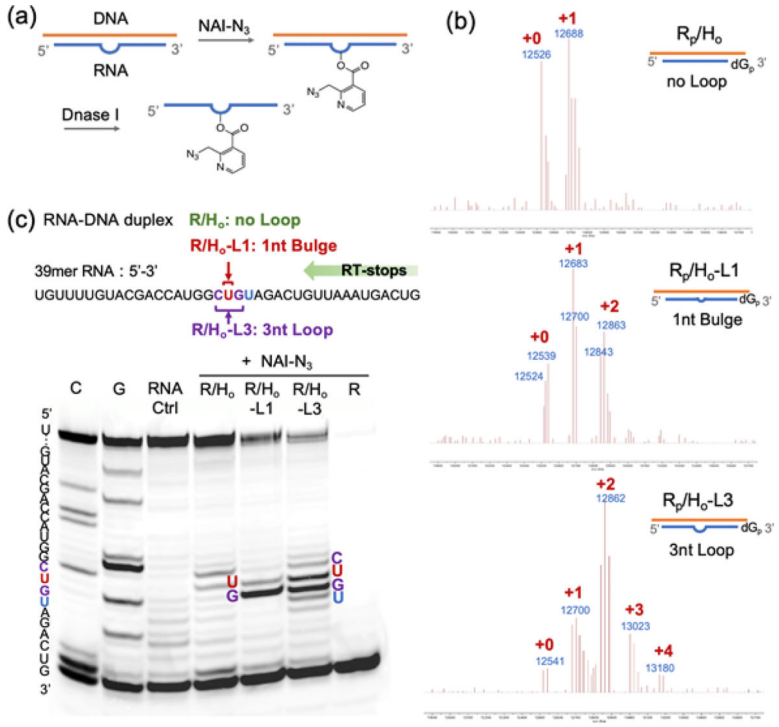

Figure 3.

Characterization of RNA acylation at DNA-induced loops. (a) Schematic showing the process of induced loop RNA acylation. (b) MALDI-TOF mass spectra of DNA-protected RNA (R_p/H_o), DNA-induced 1nt bulge RNA (R_p/H_o-L1), and DNA-induced 3nt loop RNA (R_p/H_o-L3), reacting with 200 mM NAI-N_3. (c) Gel electrophoretic analysis of RT stops for the RNA samples with no loop (R/H_o), 1nt bulge (R/H_o-L1) and 3nt loop (R/H_o-L3) reacting with 200 mM NAI-N_3. The sequence and sites of the bands in the gel are as shown. Note that RT stops (and corresponding bands) occur at the nucleotide immediately 3′ to the acylated residue.

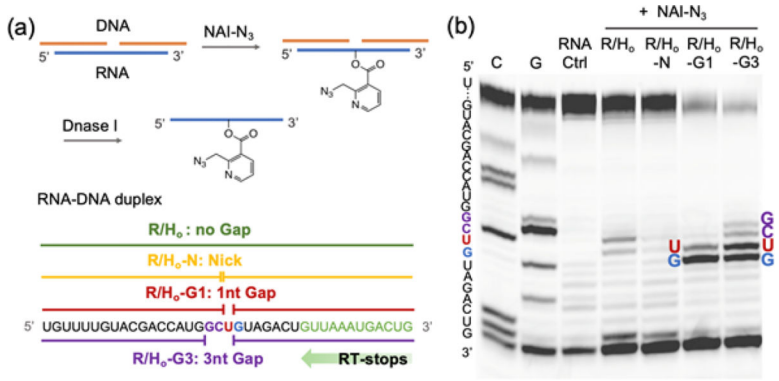

Figure 4.

Characterization of RNA acylation at induced gaps. (a) Schematic for the steps of induced-gap RNA acylation. (b) Gel electrophoretic analysis of RT stops for RNA samples with no gap (R/H_o), nick (R/H_o-N), 1nt gap (R/H_o-G1) and 3nt gap (R/H_o-G3), reacting with 200 mM NAI-N_3. Sequences and sites are as indicated.

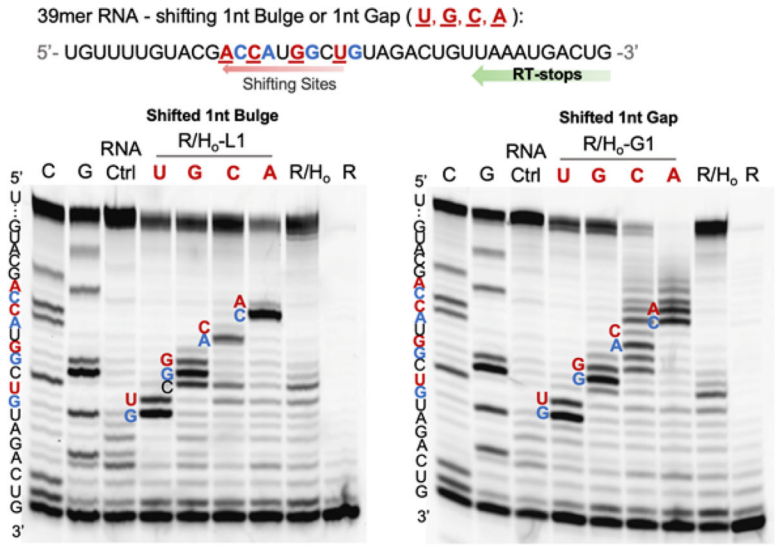

Figure 5.

Programming local acylation sites by shifting positions of loops or gaps in a 39mer RNA target. PAGE analysis of RT-stops for the samples with 1nt bulges or gaps at different positions as shown. The aligned sequences of the shifting bands in the gel are as indicated. Note that RT stops (and corresponding bands) occur at the nucleotide immediately 3′ to the reactive position.

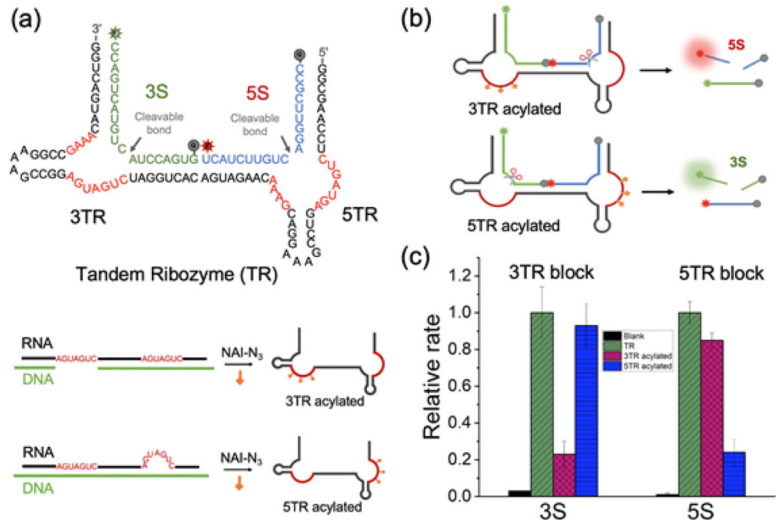

Figure 6.

RAIL approach for the site-selective programmable control of a tandem ribozyme. (a) Sequences of a tandem ribozyme (TR) with two catalytic cores (3TR, 5TR) and two dually labeled substrates of 3S for 3TR, 5S for 5TR; Selectively acylation of TR was shown on the below via RAIL method, resulting in a 3TR acylated ribozyme and a 5TR acylated ribozyme. (b) Mechanisms of RAIL method enabled site-specific control of the tandem ribozyme. (c) Plot showing the relative initial rates of each substrate (3S and 5S) cleavage relative to that of unreacted TR (normalized to 1.0). Error bars represent the standard deviation of triplicate experiments.

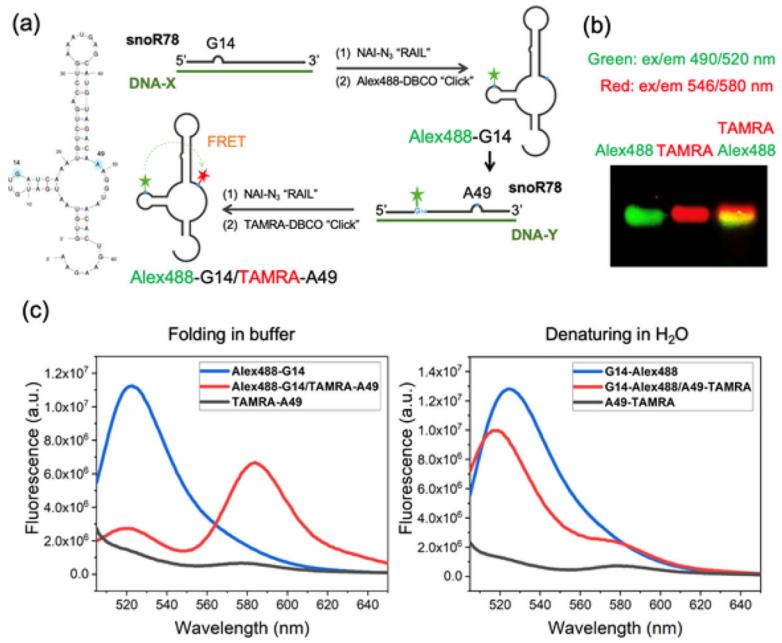

Figure 7.

Successive RAIL approach for the dual labeling of a 65nt small nucleolar RNA (SNORD78) and observation of folding by FRET. (a) SNORD78 RNA sequence with labeling sites (G14 with Alex488; A49 with TAMRA) marked in blue. Schematic for the process of RNA dual labeling via two successive reactions. (b) Image of gel analysis of double-labeled RNA; overlay of Alex488 (green) and TAMRA (red) channels showing coincidence of the two dyes. (c) FRET signals respond to changing RNA structure in buffer versus water (fluorescence emission on donor excitation at 490 nm).